

Crystallization behavior of MgO-Al₂O₃-SiO₂ glass-ceramics prepared by directly heat-treating of laterite ore smelting slag

Ning Gao, Yaxu Chen, Chengyu Wang, Yanling Guo* and Jieyu Zhang

State Key Laboratory of Advanced Special Steel, Shanghai Key Laboratory of Advanced Ferrometallurgy, School of Materials Science and Engineering, Shanghai University, Shanghai 200444, China

In this paper, we proposed a novel method to prepare MgO-Al₂O₃-SiO₂ (MAS) glass-ceramics through direct heat treatment with the slag of laterite ore. First, the Ni-Fe alloy and slag glass were prepared simultaneously by this method, and the yield rate of Ni-Fe alloy was up to 95.69%. Then, the MAS glass-ceramics can be obtained by direct heat-treating for the slag glass. The energy consumption of glass-ceramics production was much lower than that in traditional method to make full use of the thermal energy of the molten slag. The crystallization behavior of the glass-ceramics was investigated by XRD, DSC and FESEM. The results demonstrate that many phase-separated droplets appear in the slag glass. During the heat treatment, the phase-separated droplets as favorable nucleation sites to inducing crystallization. The crystallinity and crystallite size of the samples exhibits an increasing tendency with the increase of heat treatment temperature and time. The crystalline phases of glass-ceramics were two different compositions magnesium aluminum silicates (MgAl₂Si₄O₁₂ and (Mg,Al)SiO₃). The activation energies of the slag glass were calculated by Kissinger and Ozawa method, which were 308.81 and 309.36 kJ·mol⁻¹, respectively. And the crystallization mechanism of the glass-ceramics was dominated by both the surface crystallization and bulk crystallization with one-dimensional growth.

Keywords: Slag of laterite ore, Droplet phase separation, Crystallization, Glass-ceramics.

Introduction

Glass-ceramics are multi-phase composites containing microcrystalline phases and glass phases. They are made from the basic glass through crystallization heat treatment [1, 2]. Industrial solid wastes such as blast furnace slags, fly ash, BOF slag, mud resulting from hydrometallurgical processing, granite waste and mixtures of different solid wastes are widely used in the preparation of glass-ceramics [3-13]. The glass-ceramics that prepared from industrial wastes have excellent mechanical properties and good chemical resistance and have a great significance to industrial applications and environmental protection. Therefore, it has become the focus of the comprehensive utilization of slag [14-17].

The slag of laterite ore is produced during the process of nickel-iron alloy smelting from laterite ores and is a valuable resource that can be recycled and utilized containing SiO₂, Al₂O₃ and MgO. With the rapid growth in the demand for Ni-Fe alloy, the comprehensive utilization of slag has gradually attracted the attention of researchers and using this slag to prepare MAS glass-ceramics is a promising approach[18-20].

At present, most studies about the comprehensive utilization of slag focus on the second treatment of slag after the completion of the smelting process. In general, some chemical reagents or other types of solid waste are added to the original slag to adjust its composition, and then the slag glass-ceramics are obtained after high-temperature melting and heat treatment [21, 22]. However, the energy consumption and cost of this traditional treatment were very high. In contrast, the method of preparing glass-ceramics by direct heat treatment with the slag of laterite ore is more economical and environmentally friendly. This method avoids not only the addition of substances in the process of alloy smelting and slag glass-ceramic production but also the melting and reheating process of the slag. However, until now, there have been only a few reports on glass-ceramic production by direct heat treatment with the slag of laterite ore [23]. The crystallization behavior and crystallization kinetics of the resulting glass-ceramics have not been fully investigated.

In the present study, we put forward a new method for preparing MAS glass-ceramics through direct heat treatment with the slag of laterite ore. The crystallization behavior and kinetics of the glass-ceramics were investigated by differential scanning calorimetry (DSC), field-emission scanning electron microscopy (FESEM) and X-ray diffraction (XRD).

*Corresponding author:
Tel : +86-136 2184 7853
E-mail: yanling_guo@shu.edu.cn

Experimental and Characterization

Materials and experimental procedure

The laterite ore (China BaoWu Steel Group Corporation Limited) was mixed with an excess of premium grade pure carbon powder (Sinopharm Chemical Reagent Co., Ltd., China). The composition of laterite ore is shown in Table 1. A tablet press was used to apply a pressure of 10 MPa to the mixed material to turn it into a cylinder with a diameter of 50 mm to 10 mm in height. After that the material was placed in a corundum crucible and melt-reduced in a horizontal resistance furnace, The protective gas was high-purity argon.

In order to reduce the metal and obtain the Ni-Fe alloy, the sample is heated to 1200 °C and kept for one hour. In order to completely separate the slag and metal and make the liquid slag fully clarified and homogeneous, continue to heat the sample to 1500 °C for two hours. Finally, the sample furnace was cooled to room temperature and taken out. Completely separated Ni-Fe alloy and slag glass were successfully obtained (Fig. 1).

In the current slag glass system, the relative content of MgO is up to 20.3 wt.%, and a small amount of Cr₂O₃ (0.78 wt.%) and Fe₂O₃ (0.85 wt.%) also exist. Huijuan, W [24] and Rawlings, R have pointed out that these oxides can promote the crystallization of slag glass. So, in this study, a single-stage heat treatment was used as an effective method for preparing the glass-ceramics. For the purpose of studying the crystallization behaviors of glass-ceramics at different temperatures

Table 1. Chemical composition of laterite ore (wt.%)

Fe	Ni	Cr	SiO ₂	Al ₂ O ₃	MgO	CaO	LOI
26.6	1.4	1.0	29.2	7.8	7.9	0.5	13.0

and times, combining the DSC analysis results the slag glass was heat-treated at 930-1020 °C for different times (15-60 min), respectively.

Characterizations

Differential scanning calorimetry (DSC, Model-DSC404C, NETZSCH, Germany) was applied to investigate the heat variations in the samples as the temperature increased. The samples (15 ± 1 mg) was placed in a corundum crucible from ambient temperature to 1400 °C in Ar, and using Al₂O₃ as a reference material, at heating rates of 10, 15, 20 and 25 °C/min.

In order to characterize the sample, the surfaces of the sample was chemically etched with a 10% HF solution for 15s and then coated with a platinum layer. Microstructural characterization of the samples was performed using a field-emission scanning electron microscope (FESEM, Model-JSM-6700F, JEOL, Japan) with an energy dispersive spectrometer (EDS, Model-INCA, OXFORD, UK.).

The crystalline phases of the slag and glass-ceramics were examined by X-ray diffraction (XRD, Model-D\max-2550, RIGAKU, Japan). The source was Cu-K α ($\lambda = 151.5406 \text{ \AA}$), and the working voltage and tube current were 40 kV and 100 mA, respectively. The sample was scanned at an angle in the range of $10^\circ \leq 2\theta \leq 80^\circ$ at a rate of 4 °/min.

Results and discussion

Preparation and characterization of slag glass

As shown in Fig. 1, the laterite ore after the melting-reduction and cooling showed two different phases: the slag and metal spheres.

The XRD analysis for original slag and metal spheres

As shown in Fig. 1, the XRD pattern of the slag has

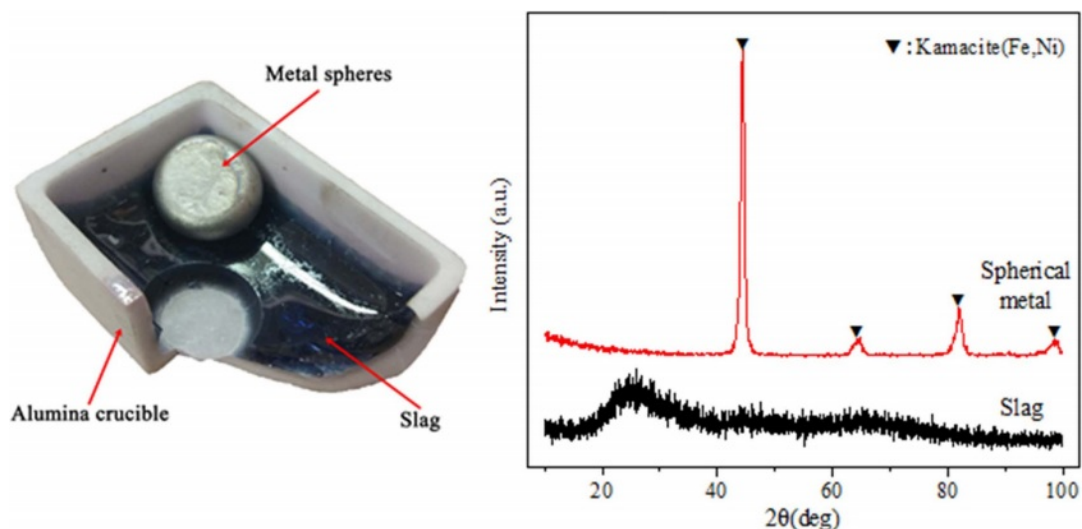


Fig. 1. The slag, metal sphere and their X-ray diffraction patterns.

typical glassy state amorphous protrusions in the range of $15^\circ \leq 2\theta \leq 35^\circ$. According to the characteristic diffraction peaks, it can be seen that the composition of the metal spheres is the kamacite phase (PDF number: 37-0474). The two different phases are slag glass and Ni-Fe alloy. what's more, the average yield of Ni-Fe alloy is 27.1 g per 100 g of laterite, and the average yield rate is 95.69%.

Microstructure of slag glass

As shown in Fig. 2(b), many phase-separated droplets with a diameter of 200~300 nm are observed in slag glass. The emergence of phase-separated droplets means the enrichment of certain elements, which changes the chemical composition of phase separation and matrix, and leads to the difference of viscosity between them. And it will affect the manner in which phase separation induces crystallization [25].

The compositions of the matrix and droplet induced crystals were characterized by EDS. The results of the EDS analysis of the micro-regions are shown in Fig. 3.

It can be seen from Fig. 3 that the enrichment of silica occurs in the crystals induced by the droplet phase and its magnesia content is lower. Thus, many

continuous silicate nets can be established in the silica-rich amorphous droplets. Mg^{2+} ($r = 0.065$ nm; the single bond strength of Mg-O = 155 kJ/mol), as a net gap ion in the glass net structure, has a great influence on the adjustment of the glass net structure and the manner of phase separation to induce crystallization. In the glass net structure, MgO can provide an O^{2-} ion to destroy the [Si-O] net structure, and Mg^{2+} can fill in the voids or gaps of the disordered net structure. Therefore, MgO breaks the chain structure of the [SiO₄] tetrahedron in the Mg-rich matrix glass, causing the viscosity of the glass matrix to decrease, the ions to easily diffuse, and the Ostwald growth (with the interfacial energy as the driving force, small particles are ablated, large particles grow, the specific mass per unit area decreases, and the total free energy of the system decreases) appears in the silica-rich droplets during the subsequent heat treatment.

Thermal analysis of slag glass

Fig. 4 shows the DSC curve of the slag glass. The slag glass transition temperature is 764 °C, the transition of atoms in slag glass and the adjustment of glass network structure at this temperature. the onset crystallization

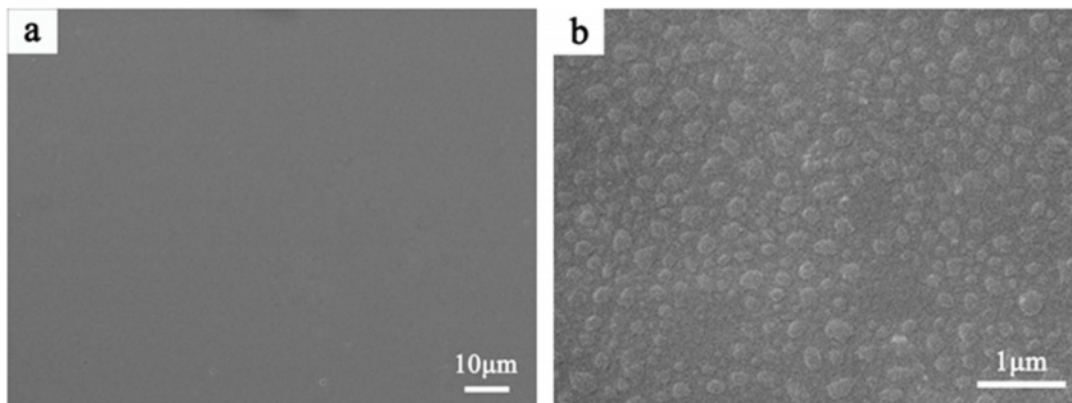


Fig. 2. SEM images of the slag glass, a: $\times 2000$; b: $\times 20000$.

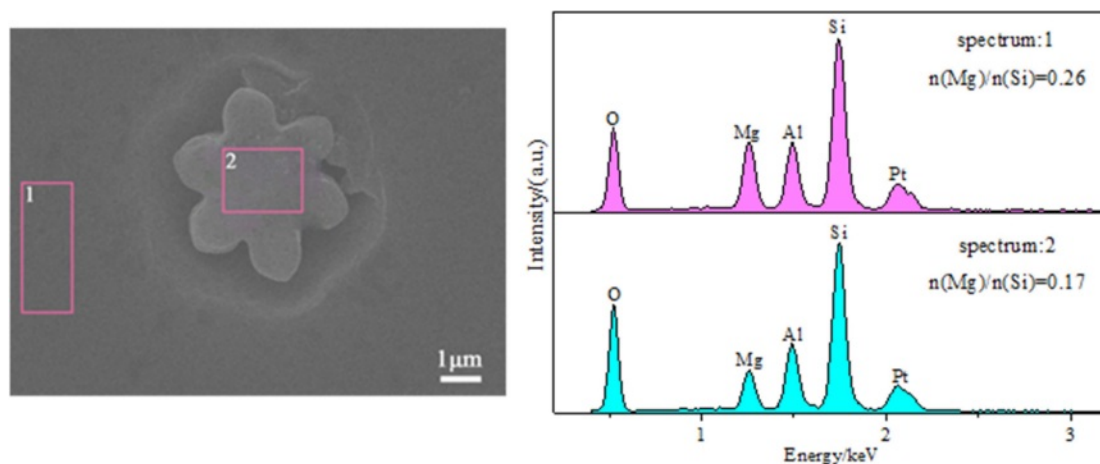


Fig. 3. EDS analyses of different phase regions in the samples (in atomic percentage).

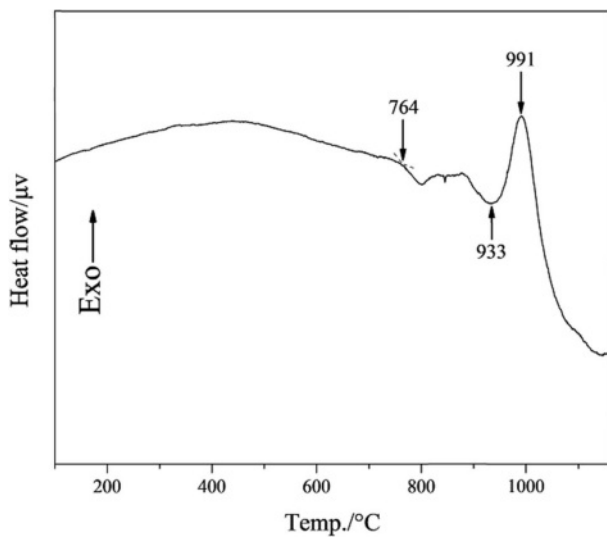


Fig. 4. DSC analysis curve of slag glass.

temperature and the crystallization peak temperature are 933 ° and 991 °.

Crystallization behavior of the glass-ceramics Heat treatment temperature

Fig. 5 shows the SEM micrographs of the samples heat treated at different temperatures for 1 h. When the heat treatment temperature is 930 or 960 °C, the number of crystals is smaller and the crystallinity of the

sample is lower. Some spherical pores of about 1.5 μm appeared in the samples. This may be due to that some of the grains are washed out by ultrasonic during the ultrasonic cleaning of the polished sample after etching in the HF solution. With the heat treatment temperature increase to 990 °C, the number and size of the crystals in the sample significantly changed. At this temperature, the viscosity of the glass is greatly reduced, and the ion diffusion rate is increased. The nucleation rate and growth rate of the crystals increase, resulting in a larger number and volume of crystals. When the heat treatment temperature was 1020 °C (Fig. 5d), the secondary growth of dendrites in the snowflake or platelet-like crystals appeared, and the length of the secondary dendrites was mainly in the range of 5-20 μm.

Fig. 6 shows the XRD patterns of the samples. After the heat treatment at 930 °C/1 h, typical glassy state amorphous protrusions appeared in the XRD pattern of this sample in the range of $15^\circ \leq 2\theta \leq 35^\circ$. Additionally, a crystalline peak of MgAl₂Si₄O₁₂ (PDF number: 27-0716) appeared at $2\theta = 25.902^\circ$. And the degree of the crystalline peak is relatively low, indicating that the number of crystals at this temperature is relatively small. After the heat treatment at 960 °C/1 h, the crystalline peak at $2\theta = 31.294^\circ$ and 35.965° indicate the appearance of another structure of magnesium aluminum silicate, (Mg,Al)SiO₃ (PDF number: 35-0310). Therefore, two kinds of crystal phases were precipitated in the sample: MgAl₂Si₄O₁₂ and (Mg,Al)SiO₃. The crystallinity

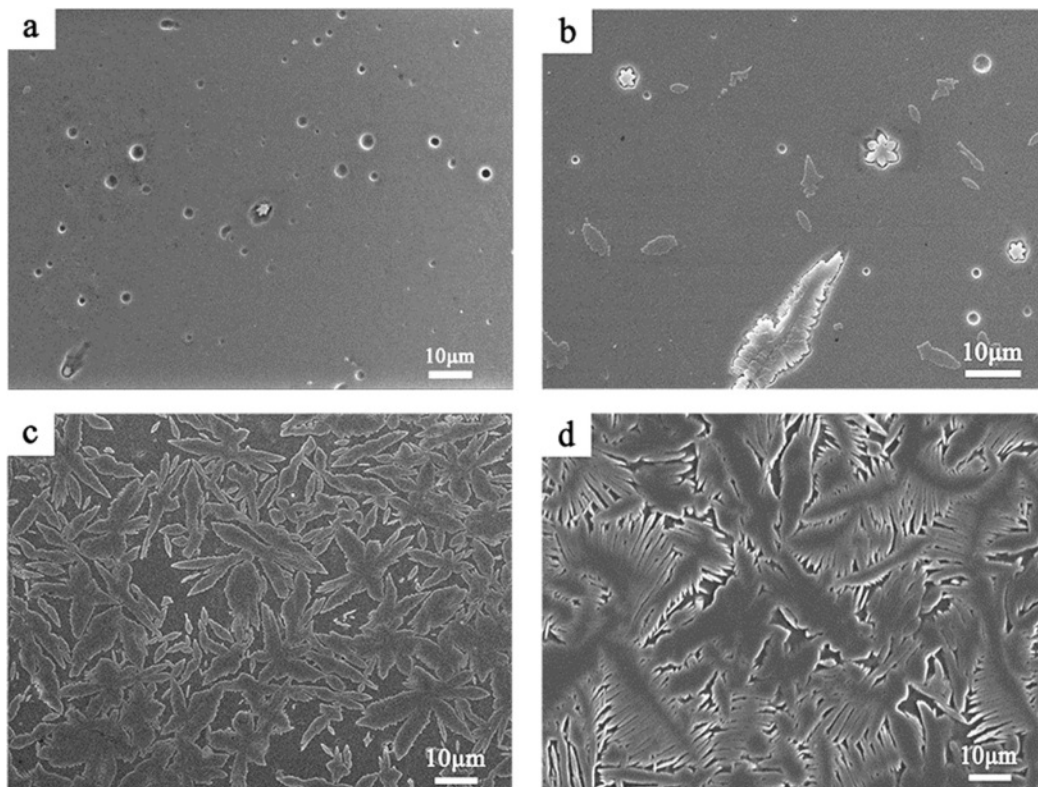


Fig. 5. SEM images of the samples (a: 930 °C/1 h, b: 960 °C/1 h, c: 990 °C/1 h, d: 1020 °C/1 h).

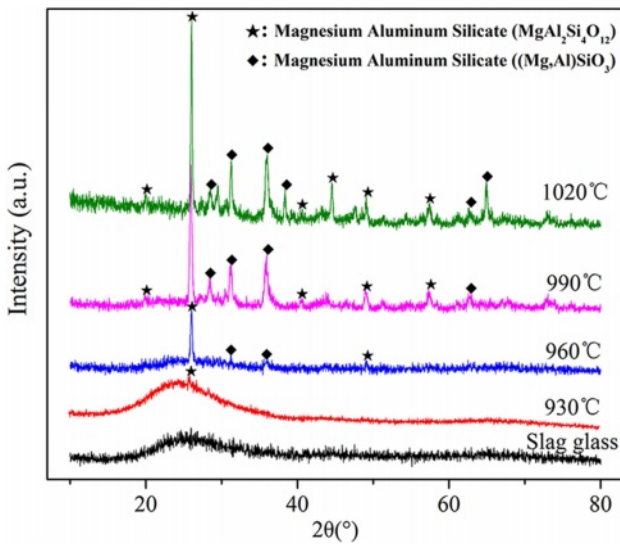


Fig. 6. XRD patterns of the samples heat-treated at different temperatures for 1 h.

of the sample was calculated to be 18.41% ($R = 6.94$) according to the crystalline peak intensity in the XRD pattern. With the heat treatment temperature increase to 990 or 1020 °C, the type of crystalline phase in the samples did not change, but the number and intensity of the crystalline peaks obviously increased. Thus, the degree of crystallization was significantly improved.

The crystallinity of the samples was calculated to be 65.63% ($R = 5.37$) and 81.72% ($R = 6.15$), respectively.

Overall, SEM images (Fig. 5) and XRD patterns (Fig. 6) demonstrate that the sample has well crystallized at 990 °C and without abnormal growth of crystals, and the crystalline phases are $MgAl_2Si_4O_{12}$ and $(Mg,Al)SiO_3$.

Heat treatment time

To further explore the effect of heat treatment time on the crystallization process of glass-ceramics, the slag glass was heat-treated at 990 °C for 15, 30, 45 and 60 min.

Fig. 7 shows the SEM images of the samples. With the heat treatment time increases, the phase-separated droplets continued to grow and accumulate to form an irregular flake- or rod-like structure. Eventually, snowflake- or flake-like crystals formed based on the mutual aggregation of irregular flake or rod-like structures. When the holding time increased from 45 to 60 min, the shape and quantity of the crystals in the sample changed significantly.

The results of the XRD patterns of the samples heat-treated at 990 °C for different times are presented in Fig. 8. The increase of heat-treatment time does not change the type of crystalline phase precipitated in the samples.

$MgAl_2Si_4O_{12}$ (PDF number: 27-0716) and $(Mg,Al)SiO_3$

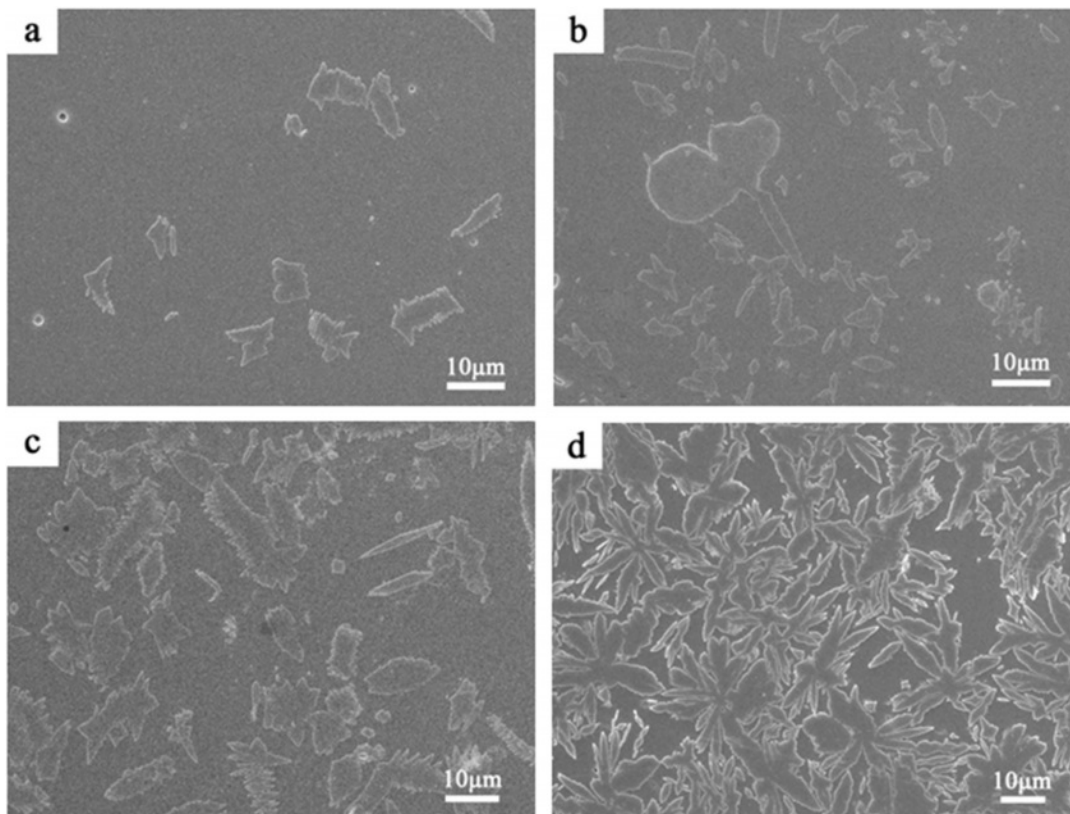


Fig. 7. SEM image of images of the samples (a: 15 min, b: 30 min, c: 45 min, d: 60 min).

(PDF number: 35-0310). Additionally, the intensity of the crystalline peaks in XRD patterns increases gradually, which means that the crystallinity of the samples is continuously increasing. The XRD patterns were refined and fitted to calculate the crystallinity. The value of R in the pattern fitting process was less than 6.5%.

Fig. 9 reveals the crystallinity of the different samples. The crystallinity increased from 2.26% to 65.63% when the heat treatment time increased. The average crystallization rate also increased as the heat treatment time increased from 15 to 60 min. This may be due to the fact that when the heat treatment temperature is in the crystallization temperature range, the viscosity of the samples decreases over time, and the ion diffusion rate increases. Therefore, when the duration of heat treatment increases from 15 to 60 min, the crystallization rate will increase gradually.

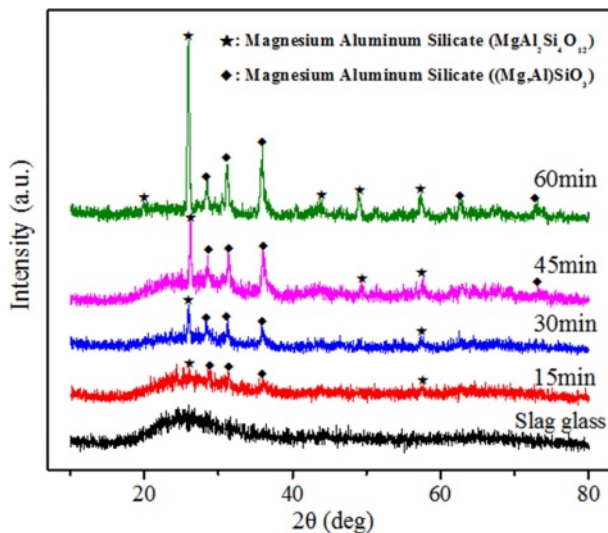


Fig. 8. XRD patterns of the samples heat-treated at 990 °C for different times.

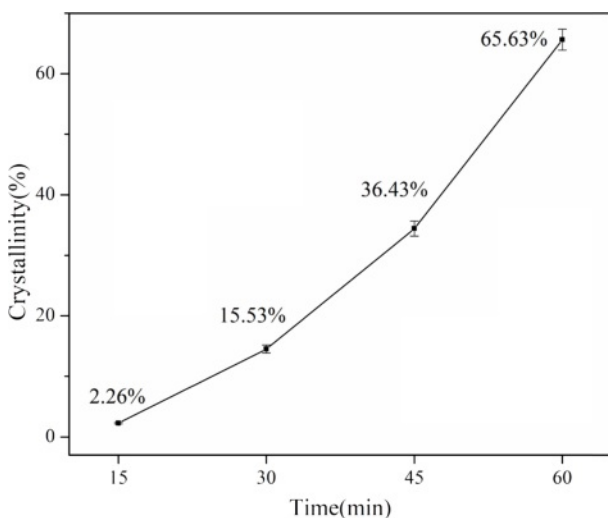


Fig. 9. Crystallinity of slag glass after heat treatment at 990 °C for different time.

Activation energy of crystallization and crystallization mechanism

At present, the Kissinger equation [26] and the Ozawa equation [27] are the commonly used methods for calculating the crystallization kinetic parameters of glass-ceramics. Zhongjie, W and El-Sheikh, S [28, 29] have successfully analyzed the crystallization kinetics of slag glass-ceramics using two methods. Consequently, in this paper, the crystallization activation energy of glass-ceramics was estimated by using the Kissinger equation and the Ozawa equation, respectively.

Kissinger equation:

$$\ln(T_p^2/\alpha) = E_C/RT_p + \text{constant} \quad (1)$$

Ozawa equation:

$$\ln \alpha = -1.502 E_C/RT_p + \text{constant} \quad (2)$$

where T_p is the crystallization peak temperature; α is the DSC heating rate, which is 10 °C, 15 °C, 20 °C, or 25 °C/min; E_C is the crystallization activation energy ($\text{J}\cdot\text{mol}^{-1}$); and R is the gas constant ($8.314 \text{ J}\cdot\text{mol}^{-1}$).

As shown in Fig. 10, the crystallization peak temperature (T_p) clearly increases with the heating rate. The value of T_p in the DSC curves at different heating rates was substituted into Eq. (1) and (2) to plot the $\ln(T_p^2/\alpha)$ vs $1/T_p$ and $\ln(\alpha)$ vs $1/T_p$ diagrams, and the data fit to a straight line. The result is shown in Fig. 11.

The values of crystallization activation energy for glass-ceramic calculated by Kissinger method and Ozawa method are $308.81 \text{ kJ}\cdot\text{mol}^{-1}$ and $309.36 \text{ kJ}\cdot\text{mol}^{-1}$, respectively. The results obtained by the two calculation methods are very similar. As reported, the crystallization activation energies of glass-ceramics prepared from blast furnace slag [30], flash furnace

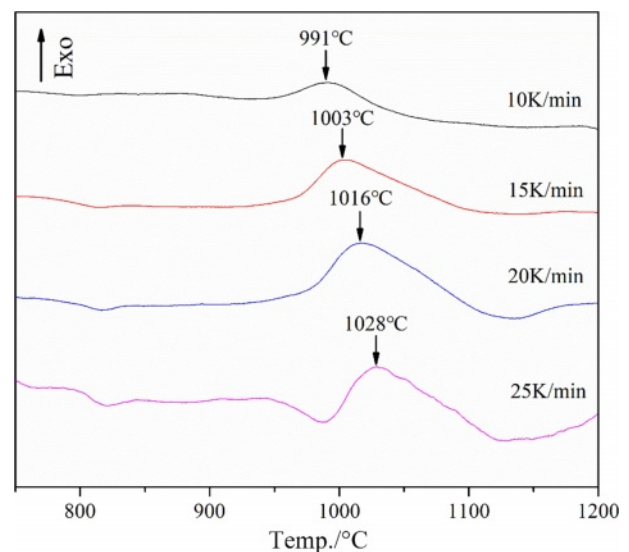


Fig. 10. DSC curves of the slag glass recorded at different heating rates.

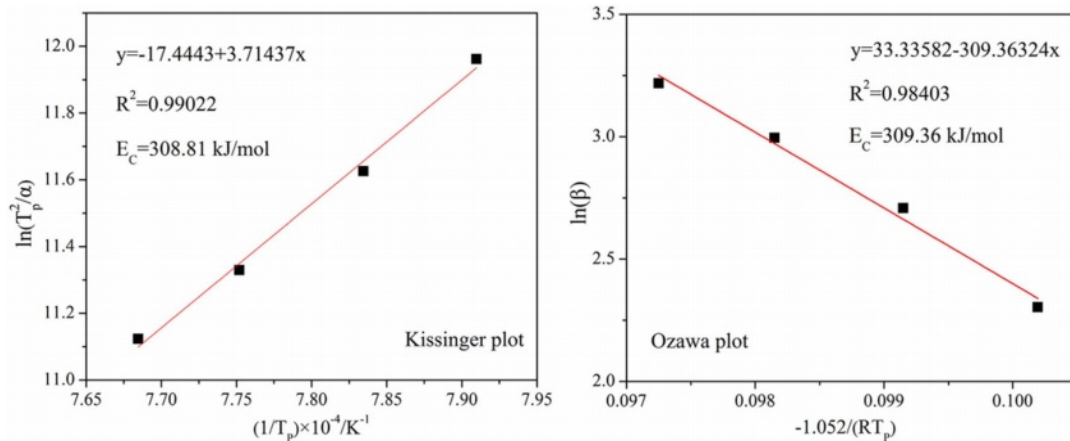


Fig. 11. Kissinger and Ozawa plots constructed from the DSC data.

Table 2. Values of the Avrami parameter (n) for various heating rates

E_C (kJ·mol ⁻¹)	Heating rate (K/min)				Average
	10	15	20	25	
308.81	1.60	1.55	1.54	1.68	1.59
309.36	1.61	1.54	1.54	1.68	1.59

nickel slag [21] and coal ash [31] are 457.5, 371.1 and 545 kJ·mol⁻¹, respectively. By comparison, the E_C of the glass-ceramic directly treated by the slag of laterite ore is smaller. In other words, the slag glass can be crystallized under low energy consumption conditions.

Subsequently, according to the calculated value of activation energy (E_C), the Avrami parameter (n) can be calculated using the equation presented by Augis, J., and Bennett, J [32]:

$$n = \frac{2.5}{\Delta T} \times \frac{RT_p^2}{E_C} \quad (3)$$

where ΔT is the width of the crystallization peak at half height. Different Avrami parameters (n) corresponded to different dimensionality of crystal growth. The value of n close to 1, 2, 3, or 4 shows that the crystallization is dominated by the surface crystallization, one-dimensional, two-dimensional, and three-dimensional growth crystallization mechanisms. The E_C obtained by the Kissinger and Ozawa methods is used to calculate the Avrami parameter (n). The results are shown in Table 2.

It can be seen from Table 2 that under different heating rates, the value of n does not change significantly. The average value of the Avrami parameter n is 1.59, indicating that the mechanism of crystallization includes the surface crystallization and the bulk crystallization with one-dimensional growth.

Conclusion

In this study, a low-cost method for preparing MAS glass-ceramics from laterite ore was introduced. The Ni-Fe alloy and the slag glass can be simultaneously obtained by adding excess carbon powder to the laterite ore and then smelting at a high temperature. Subsequently, the slag glass is heat-treated to obtain the glass-ceramic. Furthermore, the yield rate of Ni-Fe alloy is up to 95.69%, and the slag utilization rate is 100%. Obviously, this method is more economical and environmental than conventional methods.

There is significant droplet phase separation in the slag glass, which will induce the crystal to precipitate during the subsequent heat treatment. With the temperature or time increases, the crystallinity of the sample is increasing, and the type of the crystal phase does not change, that is, two different structures of magnesium aluminium silicates: MgAl₂Si₄O₁₂ and (Mg,Al)SiO₃.

Moreover, the values of crystallization activation energy for glass-ceramic calculated by Kissinger method and Ozawa method are 308.81 kJ·mol⁻¹ and 309.36 kJ·mol⁻¹, respectively. Compared with other solid waste glass-ceramics, the crystallization activation energy of the samples is smaller, and the crystallization process is easier. Furthermore, the crystallization mechanism of the glass-ceramics includes the surface crystallization and the bulk crystallization with one-dimensional growth.

Acknowledgements

This work was supported by the National Natural Science Foundation of China (No. 51304131); The Independent Research and Development Project of the State Key Laboratory of Advanced Special Steel, Shanghai University (No. SKLASS 2017-Z051); and the Shanghai Science and Technology Committee (No. YDZX20173100001316).

References

1. R. Rawlings, J. Wu, and A. Boccaccini, *J. Mater. Sci.* 41[3] (2006) 733-761.
2. J. Deubener, M. Allix, M. Davis, A. Duran, T. Höche, T. Honma, T. Komatsu, S. Krüger, I. Mitra, R. Müller, S. Nakane, M. Pascual, J. Schmelzer, E. Zanotto, and S. Zhou, *J. Non-Cryst. Solids.* 501[10] (2018) 3-10.
3. J. Kang, J. Wang, J. Cheng, J. Yuan, Y. Hou, and S. Qian, *J. Non-Cryst. Solids.* 457[1] (2017) 111-115.
4. J. Yang, D. Zhang, J. Hou, B. He, and B. Xiao, *Ceram. Int.* 34[1] (2008) 125-130.
5. K. Chen, Y. Li, Y. X. Meng, L. Meng, and Z. Guo, *Ceram. Int.* 45[18] (2019) 24236-24243.
6. D. He, C. Gao, J. Pan, and A. Xu, *Ceram. Int.* 44[2] (2017) 1384-1393.
7. M-W. Choi, and S-M. Jung, *Ironmak steelmak.* 45[5] (2018) 441-446.
8. B. Li, Z. Zhang, W. Wu, M. Zhao, Y. Shi, *IOP Conf. Ser.: Mater. Sci. Eng.* 474[1](2019) 012049.
9. C. Başaran, N. Toplan, and H. Toplan, *J. Therm. Anal. Calorim.* 134[1] (2018) 313-321.
10. T. Toya, A. Nakamura, Y. Kameshima, A. Nakajima, and K. Okada, *Ceram. Int.* 33[4] (2007) 573-577.
11. H. Liu, H. Lu, D. Chen, H. Wang, H. Xu, and R. Zhang, *Ceram. Int.* 35[8] (2009) 3181-3184.
12. E. Ljatifi, A. Kamusheva, A. Grozdanov, P. Paunovic, and A. Karamanov, *Ceram. Int.* 41[9] (2015) 11379-11396.
13. A. Demirkiran, S. Yilmaz, and U. Sen, *J. Ceram. Process. Res.* 14[1] (2013) 51-55.
14. D. Tulyaganov, M. Ribeiro, and J. Labrincha, *Ceram. Int.* 28[5] (2002) 515-520.
15. Y. Zhao, D. Chen, Y. Bi, and M. Long, *Ceram. Int.* 38[3] (2012) 2495-2500.
16. W. Dang, and H-Y. He, *J. Ceram. Process. Res.* 21[1] (2020) 69-74.
17. J. Temuujin, U. Bayarzul, E. Surenjav, K-D. Sung, and C-Y. Ski, *J. Ceram. Process. Res.* 18[2] (2017) 112-115.
18. J. Li, D. Li, Z. Xu, C. Liao, Y. Liu, and B. Zhong, *J. Clean. Prod.* 179[1] (2018) 24-30.
19. X. Ma, Z. Cui, and B. Zhao, *JOM.* 68[12] (2016) 3006-3014.
20. F. Gu, Z. Peng, Y. Zhang, H. Tang, L. Ye, W. Tian, G. Liang, M. Rao, G. Li, and T. Jiang, *ACS. Sustain. Chem. Eng.* 6[4] (2018) 4880-4889.
21. M. Mingsheng, N. Wen, and W. Yali, *J. Univ. Sci. Techno. B.* 29[2] (2007) 168-172.
22. K. Zhou, Q. Zhao, and Y. Zhang, *Univers. J. Mater. Sci.* 5[2] (2017) 52-57.
23. X. Ma, Z. Cui, and B. Zhao, *JOM-US.* 68[12] (2016) 3006-3014.
24. H. Wang, B. Li, H. Lin, W. Chen, and L. Luo, *Int. J. Appl. Glass. Sci.* 5[4] (2014) 436-442.
25. F. Xianping and C. Quanqing *J. Non-Cryst. Solids.* 112[1] (1989) 232-237.
26. H. Kissinger, *J. Res. U.S. Nat. Bur. Stand.* 57[4] (1956) 217-221.
27. C. Păcurariu, R. Lazău, I. Lazău, R. Ianoș, and B. Tița, *J. Therm. Anal. Calorim.* 97[2] (2009) 507-513.
28. Z. Wang, W. Ni, Y. Ja, L. Zhu, and X. Huang, *J. Non-Cryst. Solids.* 356[31] (2010) 1554-1558.
29. S. M. El-Sheikh, Y. M. Ahmed, E. M. Ewais, and J. F. Al-Sharab, *J. Am. Ceram. Soc.* 93[7] (2010) 2082-2091.
30. A. Francis, *J. Am. Ceram. Soc.* 88[7] (2005) 1859-1863.
31. A. Francis, R. Rawlings, R. Sweeney, and A. Boccaccini, *J. Non-Cryst. Solids.* 333[2] (2004) 187-193.
32. J. Augis, and J. Bennett, *J. Therm. Anal. Calorim.* 13 (1978) 283-292.